

Self-consistent solution of the Dyson equation for atoms and molecules within a conserving approximation

Nils Erik Dahlen^{a)} and Robert van Leeuwen

Theoretical Chemistry, Materials Science Center, Rijksuniversiteit Groningen, Nijenborgh 4, 9747 AG Groningen, The Netherlands

(Received 18 January 2005; accepted 11 February 2005; published online 25 April 2005)

We have calculated the self-consistent Green's function for a number of atoms and diatomic molecules. This Green's function is obtained from a conserving self-energy approximation, which implies that the observables calculated from the Green's functions agree with the macroscopic conservation laws for particle number, momentum, and energy. As a further consequence, the kinetic and potential energies agree with the virial theorem, and the many possible methods for calculating the total energy all give the same result. In these calculations we use the finite temperature formalism and calculate the Green's function on the imaginary time axis. This allows for a simple extension to nonequilibrium systems. We have compared the energies from self-consistent Green's functions to those of nonselfconsistent schemes and also calculated ionization potentials from the Green's functions by using the extended Koopmans' theorem. © 2005 American Institute of Physics. [DOI: 10.1063/1.1884965]

I. INTRODUCTION

Recent progress in molecular electronics has exposed the need for better theoretical methods for *ab initio* studies of nonequilibrium many-electron systems.¹ When describing transport through a single molecule one must account for the details of the electronic structure in the molecule and in the contacts. Unfortunately, the currently used theoretical methods typically predict values for the conductivity that differ by orders of magnitude from the experimentally measured values. Most of these methods aim only at describing the steady-state properties of these nonequilibrium systems, but this also requires taking the correlated dynamics of the many-electron systems into account. A first-principles description of nonequilibrium systems is highly complicated. Time-dependent density-functional theory² (DFT) offers an exact description and is also suitable for treating the quantum conduction problem.³ At present, however, density-functional calculations for quantum conduction have only been carried out at the level of the adiabatic local-density approximation,⁴ which corresponds to using exchange-correlation functionals without memory.

How to construct such improved functionals that can take dissipation properly into account is far from obvious. Solving the time-dependent Schrödinger equation for the full many-particle system is not an option due to the large computational effort. Instead, Green's-function techniques offer a natural and relatively simple method for describing a nonequilibrium correlated many-particle systems.^{5–8} Within this formalism, we can systematically improve our approximations, also including electron-phonon interactions. Compared to density-functional theory, the Green's function $G(\mathbf{r}_1 t_1, \mathbf{r}_2, t_2)$ is obviously more complicated than the electron density since it is a time-dependent function of two

coordinates. But while we know from DFT that the observables are functionals of the electron density alone, these functionals are in most cases unknown and presumably highly complicated. The same observables are simple functionals of the Green's function. Furthermore, there is no obvious path towards improved approximations in DFT, while improved approximations for the Green's functions can systematically be derived from diagrammatic techniques. In fact, the Green's-function formalism is highly useful also for deriving approximations in DFT.^{9–12}

In this paper, we will present results of Green's-function calculations for equilibrium systems as a first step towards time propagation of the full nonequilibrium Green's functions. The use of ground-state Green's-function techniques has a long history in quantum chemistry.^{13–17} The most attractive feature of this formalism is that the Green's function provides expectation values of all one-body operators, the total energy, ionization potentials, and spectral function, while being a much simpler object than the many-particle wave function. Our approach differs in two important ways from this earlier work. Firstly, we use the finite temperature formalism and calculate the Green's function on the imaginary time axis. This choice leads to a number of computational simplifications but is ultimately motivated by the possibility of easily extending the calculations to nonequilibrium systems. The second characteristic feature is that we have carried out the calculations such that the observables obtained from the Green's function agree with the macroscopic conservation laws of the underlying Hamiltonian, e.g., conservation of particle number, momentum, angular momentum, and energy. This requires the use of conserving approximations,^{18,19} a concept which is rarely discussed in quantum chemistry literature, but which is particularly important for calculations on nonequilibrium systems. Another essential part of these calculations is that the Green's func-

^{a)}Electronic mail: n.e.dahlen@rug.nl

tions should be calculated self-consistently, i.e., should not depend on a reference state. Such calculations have, to the best of our knowledge, never been carried out on molecules, though partially self-consistent solutions exist.^{15,20} If the Green's function is not self-consistent, the particle number will be incorrect,¹⁵ and the kinetic and potential energy will not be in agreement with the virial theorem. A further advantage of the conserving approximations is that the many different methods for calculating the total energy from the Green's function will give the same results.

As a first step towards studying the nonequilibrium systems, it is necessary to calculate the self-consistent Green's function of the initial equilibrium system. Such self-consistent solutions have earlier been obtained for model systems such as the homogenous electron gas²¹ and the Hubbard model,²² and lately also for the silicon crystal²³ and atoms.²⁴ While the two latter calculations aimed at calculating spectral properties and ionization potentials, we have in our calculations also been able to calculate the self-consistent total energies. We will, in the following discussions, start by briefly explaining the equations for the self-consistent Green's function, indicating which conditions must be fulfilled for obtaining physically consistent results. At the end of Sec. II, we will put our equilibrium calculations in the context of nonequilibrium many-particle physics. We will indicate there how our representation of the Green's function on the imaginary time axis corresponds to a branch of the Keldysh contour,⁵ on which the nonequilibrium Green's functions are represented. In Sec. III we will present the details on how the calculations were implemented, and self-consistent results for total energies and the ionization potentials obtained from the extended Koopmans' theorem.²⁵

II. SELF-CONSISTENT GREEN'S FUNCTIONS

We study a system in thermal equilibrium characterized by a temperature T and a chemical potential μ . Although we are here only interested in the zero-temperature limit, the finite-temperature formalism⁶ simplifies the notation and also allows for a simple generalization to time-dependent nonequilibrium systems. The equilibrium Green's function depends on the imaginary-time coordinate τ , in the range $-\beta \leq \tau \leq \beta \equiv 1/(k_B T)$, where k_B is the Boltzmann constant. With the notation $\mathbf{x} = (\mathbf{r}, \sigma)$, the Green's function $G(\mathbf{x}_1, \mathbf{x}_2; \tau)$ is a relatively simple quantity which provides a wealth of information. In particular, the one-particle density matrix is given by $\rho(\mathbf{x}, \mathbf{x}') = \lim_{\eta \rightarrow 0} G(\mathbf{x}, \mathbf{x}'; -\eta)$, and the expectation value of any one-body operator can be written according to

$$\langle \hat{O} \rangle = \text{Tr} \{ \hat{\rho} \hat{O} \} = \int d\mathbf{x} \lim_{\substack{x' \rightarrow x \\ \eta \rightarrow 0}} O(\mathbf{x}) G(\mathbf{x}, \mathbf{x}'; -\eta). \quad (1)$$

The trace indicates a summation over a complete set of states in Hilbert space and the equilibrium density operator is given by $\hat{\rho} = e^{-\beta(\hat{H} - \mu\hat{N})} / \text{Tr} \{ e^{-\beta(\hat{H} - \mu\hat{N})} \}$. From a given Green's function, there is also a large number of methods for obtaining the total energy.^{19,26} It is not automatically true that these calculated observables agree with the macroscopic conservation laws of the underlying Hamiltonian. This could, for in-

stance, mean that the trace of the density matrix gives the wrong particle number, that the energy will depend on the method used for calculating it, or that the potential and kinetic energies do not satisfy the virial theorem. We will in this paper stress the importance of calculating the Green's function from so-called conserving approximations,^{18,19} which ensures the physicality and internal consistency of the calculated observables.

Our system is described by the Hamiltonian

$$\hat{H} = \int d\mathbf{x} \psi^\dagger(\mathbf{x}) [\hat{t} + w(\mathbf{r})] \psi(\mathbf{x}) + \frac{1}{2} \int d\mathbf{x} \int d\mathbf{x}' \psi^\dagger(\mathbf{x}) \psi^\dagger(\mathbf{x}') v(\mathbf{r}, \mathbf{r}') \psi(\mathbf{x}') \psi(\mathbf{x}), \quad (2)$$

where $\hat{t} = -\nabla^2/2$ is the operator for the kinetic energy, $w(\mathbf{r})$ is the external potential and $v(\mathbf{r}, \mathbf{r}') = 1/|\mathbf{r} - \mathbf{r}'|$ is the electron interaction. We use atomic units throughout this paper. In an analogy with the Heisenberg picture, the operators are given a time dependence according to $\hat{O}_H(\tau) = e^{\tau(\hat{H} - \mu\hat{N})} \hat{O} e^{-\tau(\hat{H} - \mu\hat{N})}$. The Green's function is then defined as the expectation value

$$G(\mathbf{x}_1 \tau_1, \mathbf{x}_2 \tau_2) = \langle T [\hat{\psi}_H(\mathbf{x}_1 \tau_1) \hat{\psi}_H^\dagger(\mathbf{x}_2 \tau_2)] \rangle = \theta(\tau_1 - \tau_2) \langle \hat{\psi}_H(\mathbf{x}_1 \tau_1) \hat{\psi}_H^\dagger(\mathbf{x}_2 \tau_2) \rangle - \theta(\tau_2 - \tau_1) \langle \hat{\psi}_H^\dagger(\mathbf{x}_2 \tau_2) \hat{\psi}_H(\mathbf{x}_1 \tau_1) \rangle, \quad (3)$$

where $\hat{\psi}_H(\mathbf{x}\tau)$ and $\hat{\psi}_H^\dagger(\mathbf{x}\tau)$ are field annihilation and creation operators in the Heisenberg picture. The time-ordering operator T moves the operator with the largest time argument to the left. The equilibrium Green's function depends only on the difference between the two time coordinates, and we can thus write $G(\mathbf{x}_1 \tau_1, \mathbf{x}_2 \tau_2) = G(\mathbf{x}_1, \mathbf{x}_2; \tau_1 - \tau_2)$. The Green's function solves the equation of motion

$$\left[-\partial_\tau + \frac{\nabla^2}{2} - w(\mathbf{r}) - v_H(\mathbf{r}) + \mu \right] G(\mathbf{x}, \mathbf{x}'; \tau) = \delta(\tau) \delta(\mathbf{x} - \mathbf{x}') + \int_0^\beta d\tau_1 \int d\mathbf{x}_1 \Sigma(\mathbf{x}, \mathbf{x}_1; \tau - \tau_1) \times G(\mathbf{x}_1, \mathbf{x}'; \tau_1), \quad (4)$$

where the Hartree potential $v_H(\mathbf{r})$ and the self-energy $\Sigma(\mathbf{x}, \mathbf{x}'; \tau)$ account for the effects of the electron-electron interaction. Both the Hartree potential and the self-energy are functionals of the Green's function, which means that the Dyson equation [Eq. (4)] should be solved to self-consistency. The self-energy functional must be approximated, but for any approximation beyond Hartree-Fock the computational effort involved in solving this equation is rather larger. Self-consistent calculations for real systems have only recently appeared.²³ Earlier calculations on molecules and atoms have, however, obtained partially self-consistent solutions.^{15,20}

While we in this paper are concerned with atoms and small molecules at zero temperature, the calculations will have to be carried out at a finite temperature. The temperature must be low enough such that we can clearly distinguish between occupied states with energies below the chemical

potential and unoccupied states with energies below the chemical potential. This presents no problem for systems with a finite highest occupied molecular orbital-lowest unoccupied molecular orbital (HOMO-LUMO) gap, and the exact value of the chemical potential μ is not important as long as the value is in the gap. In the zero-temperature limit, shifting the chemical potential by a small value will obviously change the Green's function, but not the value of the observables.

Expanding the Green's function in a one-particle basis $\{\phi_i(\mathbf{x})\}$, the Dyson [Eq. (4)] becomes an equation to the time-dependent matrix $G_{ij}(\tau)$. It is convenient to write the Green's function on the form $G_{ij}(\tau) = \theta(\tau)G_{ij}^>(\tau) + \theta(-\tau)G_{ij}^<(\tau)$, as indicated in Eq. (3). This notation clearly displays the discontinuity of the Green's function at $\tau=0$ given by

$$\lim_{\tau \rightarrow 0} [G_{ij}(\tau) - G_{ij}(-\tau)] = [G_{ij}^>(0) - G_{ij}^<(0)] = -\delta_{ij}. \quad (5)$$

To solve Eq. (4) we also need the boundary condition $G_{ij}(\tau - i\beta) = -G_{ij}(\tau)$, which expresses that the Green's function is antiperiodic in the τ variable.²⁷ This follows from the definition of the Green's function in Eq. (3). To illustrate these and other properties of the Green's function, it is useful to consider a noninteracting Green's function G^0 , which results from approximating the self-energy Σ with a τ -independent one-particle potential. Finding the Green's function then corresponds to solving a set of one-particle equations. Using the corresponding orbitals as eigenfunctions, G^0 is diagonal and given in terms of the eigenvalues ϵ_i according to⁶

$$G_{ij}^{0,<}(\tau) = \delta_{ij} n(e_i) e^{-\tau e_i} \quad (6a)$$

$$G_{ij}^{0,>}(\tau) = -\delta_{ij} [1 - n(e_i)] e^{-\tau e_i}. \quad (6b)$$

Here, $e_i = \epsilon_i - \mu$, and the term $n(e) = 1/(e^{\beta e} + 1)$ is the Fermi distribution. The fact that G^0 is antiperiodic and has the discontinuity [Eq. (5)] is easily verified. We now see that if $\beta \rightarrow \infty$, then $G_{ii}^{0,<}(0) = -G_{ii}^{0,>}(\beta) = 1$ if $\epsilon_i < \mu$, and 0 if $\epsilon_i > \mu$. Conversely, we have $G_{ii}^{0,<}(-\beta) = -G_{ii}^{0,>}(0) = 0$ if $\epsilon_i < \mu$, and 1 otherwise. Due to the exponential dependence on τ , the Green's function will be peaked around the times $\tau=0$ and $\tau=\pm\beta$. This is true also for the fully interacting Green's function as well as the self-energy $\Sigma(\tau)$, although the values at the endpoints will then not be exactly 0 and 1.

We will in the following consider unpolarized systems, such that $\phi_{i\uparrow} = \phi_{i\downarrow} \equiv \phi_i$. While the Dyson equation [Eq. (4)] is exact, the self-energy $\Sigma[G]$ must be approximated in practical calculations. In these calculations we have chosen to use the second-order approximation to the self-energy, as illustrated in Fig. 1. Since the electron interaction is instantaneous, this self-energy has a particularly simple form. The first diagram in Fig. 1 is the exchange diagram,

$$\Sigma_{x,ij}(\tau) = -2\delta(\tau) \sum_{kl} G_{kl}^<(0) v_{iklj}, \quad (7)$$

where the two-electron integrals are here defined according to

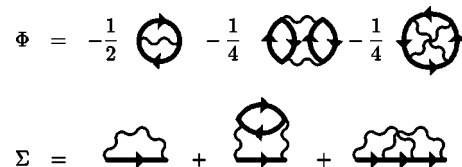


FIG. 1. The second-order approximation to the self-energy Σ can be derived as a functional derivative of a functional Φ . The first diagram of Φ and Σ are the exchange-energy and self-energy diagrams, respectively.

$$v_{ijkl} = \int d\mathbf{r} \int d\mathbf{r}' \phi_i^*(\mathbf{r}) \phi_j^*(\mathbf{r}') v(\mathbf{r} - \mathbf{r}') \phi_k(\mathbf{r}') \phi_l(\mathbf{r}). \quad (8)$$

The two remaining diagrams represent the correlation contribution.

$$\Sigma_{c,ij}(\tau) = - \sum_{klmnpq} G_{kl}(\tau) G_{mn}(\tau) G_{pq}(-\tau) \times v_{iqmk} [2v_{lnpj} - v_{nlpj}]. \quad (9)$$

The factor 2 that appears in Eqs. (7) and (9) comes from summing over the spin indices. It can be shown that both the Green's function and the self-energy are real, symmetric, τ -dependent matrices. The second-order diagrams resemble those evaluated in second-order Møller–Plesset perturbation theory.¹⁵ The most important difference between our calculations and second-order perturbation theory is that we solve the Dyson equation to self-consistency, and the final result is, for this reason, independent of any reference state. It also means that the self-energy [Eq. (9)] is evaluated using a non-diagonal Green's function matrix.

The second-order approximation is an example of a conserving approximation,^{18,19} which means that the self-energy can be obtained as the functional derivative of a functional $\Phi[G, v]$,

$$\Sigma(\mathbf{x}, \mathbf{x}'; \tau) = \frac{\delta\Phi}{\delta G(\mathbf{x}', \mathbf{x}; -\tau)}. \quad (10)$$

The Φ functional corresponding to the second-order approximation is shown in Fig. 1. The observables calculated from the Green's function will then agree with the macroscopic conservation laws of the underlying Hamiltonian. The Hartree potential is also a functional of the Green's function since the density given by $n(\mathbf{x}) = \rho(\mathbf{x}, \mathbf{x}) = \lim_{\eta \rightarrow 0} G(\mathbf{x}, \mathbf{x}; -\eta)$. In calculations, one will start with an initial guess for G , e.g., the Hartree–Fock (HF) Green's function on the form indicated in Eq. (6). One then calculates the Hartree potential and the self-energy from Eqs. (7) and (9) and solves the Dyson equation [Eq. (4)]. If the self-consistency cycle is not continued, the resulting observables will depend on the initial Green's function. The results can be unphysical and can produce e.g., an incorrect particle number. Partial self-consistency, which means that the correlation part of the self-energy [Eq. (9)] is fixed while the Hartree–Fock potential $v_H + \Sigma_x$ is updated, can significantly improve the results¹⁵ but will, in general, not remove the unphysical features of the calculated observables.

Another advantage of self-consistent calculations, is that all the various methods for calculating the total energy from the Green's function give the same result (for a detailed dis-

discussion, see Refs. 19 and 26). The most straightforward of these methods is to evaluate the individual energy terms,

$$E = T + V_{ne} + V_{ee} + V_{nn}, \quad (11)$$

where the kinetic energy T and the nuclear-electron attraction energy V_{ne} are trivially obtained from the density matrix. The electron interaction energy is $V_{ee} = U_0 + U_{xc}$, where $U_0 = 1/2 \int d\mathbf{r} d\mathbf{r}' n(\mathbf{r}) v(\mathbf{r}, \mathbf{r}') n(\mathbf{r}')$ is the Hartree energy, and the exchange and correlation energy can be calculated from the expression

$$U_{xc} = \frac{1}{2} \int_0^\beta d\tau \sum_{ij} \sum_{ij} (-\tau) G_{ji}(\tau). \quad (12)$$

When the Green's function is obtained from a conserving approximation, the kinetic and potential energy will agree with the virial theorem (see Appendix) such that $2T = -V_{ne} - V_{ee} - V_{nn}$.

The Green's functions have frequently been used to obtain removal and addition energies, since these correspond to poles in the Fourier-transformed Green's function, $G(\omega) = \int dt G(t) e^{i\omega t}$, where the time variable t corresponds to a real-time variable.⁶ Such calculations have recently been carried out on atoms,²⁴ where the Green's function was calculated self-consistently from a self-energy with a dynamically screened coulomb interaction (the GW approximation.²⁸) the one-particle Green's function with screened coulomb interaction (GW) approximation.²⁸ In the present work, we have employed the finite-temperature formalism and the Green's function is represented on the imaginary rather than on the real-time axis. The Fourier transform of the real-time Green's function can be obtained from the Fourier transform of the Green's function for imaginary times, $G(i\omega_n) = \int_0^\beta d\tau G(\tau) e^{i\omega_n \tau}$, by analytic continuation. Such calculations have been done for the silicon crystal,²³ where the Green's function was obtained on the imaginary time axis, and the Fourier transform $G(\omega)$ was found from $G(i\omega)$ by the use of Padé approximations.

For our calculations we have not found this approach practical. We have instead chosen to calculate ionization potentials from the extended Koopmans' Theorem (EKT).²⁵ The ionization potentials are found from the eigenvalue equation

$$\sum_{ij} \Delta_{ij} u_j^m = (E_0^N - \mu N - \lambda_m) \sum_j \rho_{ij} u_j^m, \quad (13)$$

where the matrix Δ is defined according to

$$\Delta_{ij} = \int d\mathbf{x} \int d\mathbf{x}' \phi_j(\mathbf{x}) \langle \hat{\psi}^\dagger(\mathbf{x}) [\hat{\psi}(\mathbf{x}'), \hat{H} - \mu \hat{N}] \phi_i^*(\mathbf{x}') \rangle. \quad (14)$$

This definition differs from the one found in Ref. 25 by the inclusion of the chemical potential. Using the definition of the Green's function in Eq. (3) and the Dyson equation [Eq. (4)], we can write Δ and the density matrix ρ as

$$\Delta_{ij} = -\partial_\tau G_{ij}(\tau)|_{\tau=0^-} \quad \text{and} \quad \rho_{ij} = G_{ij}(0^-). \quad (15)$$

We now interpret the eigenvalues λ_m as the energies of the $N-1$ particle system, $\lambda_m = E_m^{N-1} - \mu(N-1)$. For the second-

order approximation, the self-consistent Green's function is real and symmetric, which implies that both the matrices Δ and ρ are symmetric. The eigenvalue problem can therefore be rewritten according to

$$\sum_{ij} \tilde{\Delta}_{ij} \tilde{u}_j^m = -\tilde{\lambda}_m \tilde{u}_i^m, \quad (16)$$

where $\tilde{\Delta}_{ij} = (\rho^{-1/2} \Delta \rho^{-1/2})_{ij}$ and $\tilde{u}_i^m = \sum_j (\rho^{1/2})_{ij} u_j^m$. The eigenvalues give the EKT ionization potentials according to $\tilde{\lambda}_m = \lambda_m - E_0^N + \mu N = \mu + E_m^{N-1} - E_0^N = I_m^{\text{EKT}} + \mu$.

As we mentioned in the Introduction, one of the main reasons why we choose to work in the finite-temperature formalism is that the equations can easily be generalized to nonequilibrium systems. For a system initially in equilibrium at $t=0$, the time-dependent value of the expectation value is given by $\langle \hat{O} \rangle(t) = \text{Tr}\{\hat{\rho} \hat{O}_H(t)\}$, where the subscript H indicates the Heisenberg picture. The time-dependence of the operator is given by the evolution operators $\hat{O}_H(t) = \hat{U}(0, t) \hat{O} \hat{U}(t, 0)$, where $i\partial_t \hat{U}(t, t') = \hat{K}(t) \hat{U}(t, t')$, and we have defined $\hat{K}(t) = \hat{H}(t) - \mu \hat{N}$. Since the equilibrium density operator $\hat{\rho}$ can also be written as an evolution operator, $\hat{\rho} = \hat{U}(-i\beta, 0) / \text{Tr}\{U(-i\beta, 0)\}$, the time-dependent expectation value of the operator \hat{O} can be written as

$$\langle \hat{O} \rangle(t) = \frac{\text{Tr}\{\hat{U}(-i\beta, 0) \hat{U}(0, t) \hat{O} \hat{U}(t, 0)\}}{\text{Tr}\{U(-i\beta, 0)\}}. \quad (17)$$

The numerator, read from right to left, describes an evolution along a time contour from the initial time 0 to t , then back to 0, and along the imaginary time axis to $-i\beta$. This introduces the concept of the Keldysh time contour,⁵ which is central to the study of nonequilibrium system. A nonequilibrium system at a time t can now be described by a Green's function $G(\mathbf{x}_1 t_1, \mathbf{x}_2 t_2)$, where the time arguments must be located on this contour starting at 0, passing through t , and ending at $-i\beta$. In calculations, this means that we will first calculate the Green's function for time arguments on the imaginary axis in order to describe the initial equilibrium systems. The time evolution then implies extending the contour on which the Green's function is defined along the real axis, starting from $t=0$. Our calculations therefore constitute the first step in the propagation of the nonequilibrium Green's functions. This method is also a direct way of obtaining the equilibrium Green's function on the real time axis rather than on the imaginary time axis. This is simply done by propagating the Green's function along the real time axis, without any additional time-dependent potential. The resulting Green's function will only depend on the difference $t_1 - t_2$ between the time coordinates, and will essentially be equivalent to ordinary real-time Green's function.

III. RESULTS

The calculations were carried out using a set of Slater basis functions, using 25 basis functions for each hydrogen atom and 30–40 basis functions for each of the other atoms.²⁹ As the Green's function is peaked around the endpoints $\tau=0$ and $\tau=\pm\beta$, it is inconvenient to represent the

TABLE I. Energies calculated from the self-consistent Green's function and from the Luttinger–Ward functional evaluated at the HF and LDA Green's functions. The term U_c denotes the correlation part of the interaction energy. The energy $E[G^2]$ is calculated from the second-order (non-selfconsistent) Green's function. All energies are in hartrees. The H_2 calculation was carried out for internuclear separation $R=1.4$, while the separation was $R=3.015$ for LiH.

	T	V_{ne}	U_c	V_{ee}	E	$E_{LW}^2[G_{HF}]$	$E[G^2]$	E_{HF}
He	2.8981	-6.7585	-0.0703	0.9635	-2.8969	-2.8969	-2.9013	-2.8617
Be	14.6362	-33.6781	-0.1367	4.4009	-14.6409	-14.6405	-14.6662	-14.5728
Ne	128.8790	-311.1072	-0.5748	53.3944	-128.8339	-128.8332	-128.7979	-128.54704
Mg	199.8400	-479.0677	-0.5937	79.3181	-199.9097	-199.9093	-199.9279	-199.6146
Mg ²⁺	199.0333	-469.8175	-0.5489	71.6822	-199.1020	-199.1025	-199.0754	-198.8305
H ₂	1.1600	-3.6463	-0.0645	0.6062	-1.1659	-1.1658	-1.1722	-1.1336
LiH	8.0488	-20.4673	-0.1294	3.3746	-8.0515	-8.0513	-8.0608	-7.9868

Green's function on an even-spaced time grid. We have therefore used the uniform power mesh method, as described in Ref. 23, which is dense only at the end points 0 and $\tau = \pm\beta$. It is usually sufficient to have between 40 and 80 points on the time mesh. The first step in the calculations consists of solving the HF or DFT equations, resulting in an initial Green's function $G^0(\tau)$. Using the orbitals with eigenvalues ϵ_i as basis functions, this Green function matrix is diagonal and has the form

$$G_i^0(\tau) = \theta(\tau)(n(\epsilon_i) - 1)e^{-\epsilon_i\tau} + \theta(-\tau)n(\epsilon_i)e^{-\epsilon_i\tau}. \quad (18)$$

We have again used the notation $e_i = \epsilon_i - \mu$, subtracting the chemical potential μ from the HF or DFT eigenvalues. In our calculations, the inverse temperature was set to $\beta=100$, which is sufficiently low to approximate the zero-temperature limit. Only if the HOMO-LUMO gap becomes very narrow, as for an H₂ molecule at large internuclear separations, must the temperature be set lower in order to clearly distinguish between occupied and unoccupied levels. The exact location of the chemical in the HOMO-LUMO gap is otherwise arbitrary. We can shift the chemical potential (equivalent to shifting the eigenvalues ϵ_i) without changing the properties of the system, as long as the eigenvalues of the occupied states are negative and the eigenvalues of the unoccupied states are positive.

The noninteracting Green's function corresponds to a solution of the noninteracting Dyson equation,

$$[-\partial_\tau - h_{ij}]G_j^0(\tau) = \delta_{ij}\delta(\tau) + \sum_k \Sigma_{ij}^0 G_k^0(\tau). \quad (19)$$

The self-energy matrix Σ_{ij}^0 equals $\int dx \phi_i^*(x)v_{Hxc}(x)\phi_j(x)$ if the orbitals are obtained from a DFT calculation, or $\int dx \int dx' \phi_i^*(x)v_{HF}(x, x')\phi_j(x')$ if the orbitals are obtained from a HF calculation. From this initial Green's function, we can solve the Dyson equation on the integral form,

$$G_{ij}(\tau) = \delta_{ij}G_i^0(\tau) + \int_0^\beta d\tau_1 \int_0^\beta d\tau_2 \sum_k G_i^0(\tau - \tau_1) \times \tilde{\Sigma}_{ik}(\tau_1 - \tau_2)G_{kj}(\tau_2), \quad (20)$$

where $\tilde{\Sigma}_{ik}(\tau_1 - \tau_2) \equiv \Sigma_{ik}(\tau_1 - \tau_2) - \delta(\tau_1 - \tau_2)\Sigma_{ik}^0$. For a given Σ , solving the Dyson equation [Eq. (20)] for G means having to solve a set of linear equations, which can be done by using iterative methods such as, e.g., the biconjugate gradient

method. This is somewhat more complicated than the conventional procedure of solving the Dyson equation for the Fourier-transformed function $G(\omega)$, when the time convolution integrals transform into products of the Fourier-transformed functions. While representing the functions in frequency space is convenient when not attempting to find a self-consistent solution, the discontinuities at the points $t = 0$ and $\pm\beta$ makes this inconvenient for our calculations. The frequency space representation has the additional problem that the functions decay slowly as a function of ω , which causes frequency integrals to converge very slowly.

Having solved Eq. (20), the self-energy Σ must now be calculated with this new G , for which a new solution of Eq. (20) must be obtained. This procedure will eventually lead to a self-consistent Green's function. It is important to stress that while the reference functions G^0 and Σ^0 appear in the Dyson equation [Eq. (20)], the observables obtained from the self-consistent Green's function should not depend on the choice of reference state, as is also indicated by Eq. (4). Using orbitals from the local density approximation (LDA) or HF, orbitals should lead to the same result (i.e., the observables calculated from the Green's function should be the same). Solving the Dyson equation for different choices of Σ^0 can therefore serve as a useful numerical test of the calculations (in particular, for checking whether the number of points of the time mesh is large enough). We have found that convergence is reached much more quickly when using HF rather than DFT as starting point.

The self-consistent energies are shown in Table I. We have also included the HF energies and the total energy calculated from the Luttinger–Ward (LW) functional.^{30–32} The LW functional $E_{LW}[G]$ is a functional of the Green's function, such that $\delta E[G]/\delta G=0$ when G is the self-consistent solution of the Dyson equation. At the self-consistent G , the LW functional gives exactly the same result as the methods discussed above. Evaluating the LW functional on an approximate noninteracting Green's function such as, e.g., the HF Green's function then yields energies close to the self-consistent values due to the variational property of the energy functional. That this is indeed the case can be seen in Table I, where the deviation between the LW energies and the self-consistent results are less than one millihartree. This illustrates the fact that the functional is indeed insensitive to the input of Green's function, and that a very good estimate

TABLE II. Ionization potentials calculated from the extended Koopmans' theorem. The results in the first column are calculated from the self-consistent Green's function, while those in the column labeled EKT[G^2] are calculated from the Green's function obtained from the first iteration of Eq. (20). The HF values correspond to the HF eigenvalues.

	EKT[G]	EKT[G^2]	HF	Expt.
He	0.9017	0.9059	0.9181	0.9036 ^a
Be	0.3130	0.3275	0.3084	0.3426 ^a
Ne	0.7412	0.7363	0.8504	0.7925 ^a
Mg	0.2548	0.2605	0.2530	0.2810 ^a
H ₂	0.5921	0.5999	0.5947	0.5669 ^b
LiH	0.2884	0.2942	0.3015	0.2903 ^c

^aFrom Ref. 34.

^bFrom Ref. 35.

^cFrom Ref. 36.

for the self-consistent energies can be obtained without having to solve the Dyson equation. As can be seen from the table, the virial theorem is satisfied reasonably well. The deviation of the kinetic from the negative of the total energy is due to the limited size of the basis sets and becomes smaller when increasing the number of basis functions.

The advantage of self-consistent calculations is that the results depend only on the chosen diagrammatic approximation and not on the reference state. In Ref. 30, we showed how the LW energies are also very close to the conventional second-order Møller–Plesset (MP2) energies, and according to the results in Table I, the MP2 energies are thus also very close to the self-consistent energies. This is interesting, since the Møller–Plesset series can be shown to diverge,³⁵ while the self-consistent Green's function calculations take into account contributions to infinite order in the electron interaction. We can expect to see a large difference between the MP2 energy and the self-consistent results in systems where MP2 fails badly, e.g., for the dissociation curve of the H₂ molecule. While the MP2 energy diverges when the internuclear separation $R \rightarrow \infty$, the first iteration of the Dyson equation [Eq. (20)] yields a finite result.¹⁵

In addition to results obtained from the self-consistent Green's function, we have also included non-self-consistent results. These are calculated using a Green's function obtained from solving the Dyson equation [Eq. (20)] only once, with Σ^0 and G^0 equal to the HF self-energy and Green's function. This means that G^2 solves the equation (skipping the indices and the time coordinates for notational simplicity)

$$G^2 = G_{\text{HF}} + G_{\text{HF}} \Sigma_c [G_{\text{HF}}] G^2, \quad (21)$$

where Σ_c is given by Eq. (9), evaluated with the HF Green's function. We have also included the HF eigenvalues, corresponding to the conventional Koopmans' theorem. The results clearly show that iterating the Dyson equation to self-consistency significantly changes the ionization potentials.

In Table II we list ionization potentials calculated from the EKT. Also the ionization potentials depend significantly on whether the calculations are carried out to self-consistency or not. The ionization potentials are in agreement with the preliminary results we have obtained from real-time propagation.

IV. CONCLUSIONS

The use of conserving approximations is essential not only when considering time-dependent systems, but also for systems in the ground state. The concept of conserving approximations implies finding a self-consistent solution to the Dyson equation. While this increases the computational effort, the results are unambiguous in the sense that the resulting observables are internally consistent and independent both of reference state and of the particular method used for calculating them from the Green's function. We have found it useful to confirm that the self-consistent total energies are in very good agreement with those obtained from the Luttinger–Ward functional. This means that it is possible to estimate the merits of a certain diagrammatic approximations without actually performing the self-consistent calculation of the Green's function. For calculating anything else than the total energy, one still needs to carry out the full calculations.

Using the finite-temperature formalism to represent the Green's function on an imaginary time axis simplifies the calculation of observables from the Green's function, since we avoid performing the slowly converging frequency integrals that appear when using the Fourier-transformed quantities. But the most important reason for calculating the Green's function on the imaginary time axis is that this is the obvious starting point for treating the system out of equilibrium. We should here point out that a very good approximation to the self-consistent Green's function can be obtained by updating only the static part of the self-energy, $v_H + \Sigma_x$, while letting the correlation part be calculated from the HF Green's function, i.e., $\Sigma_c = \Sigma_c [G_{\text{HF}}]$. This calculation is significantly faster than the fully self-consistent procedure, but is not relevant when considering nonequilibrium systems. The reason for this is that while the self-consistent Green's function in the ground state remains largely diagonal in the HF basis functions, the off-diagonal terms become significant when the system is disturbed. The truly nonequilibrium case will be part of a future publication.

ACKNOWLEDGMENTS

We thank Ulf von Barth and Thijs Holleboom for stimulating discussions.

APPENDIX: THE VIRIAL THEOREM

We will in the following show that a self-consistent Green's function obtained from a conserving approximation produces energies in agreement with the virial theorem. As shown by Baym,¹⁹ a conserving self-energy corresponds to a functional derivative of a functional $\Phi[G, v]$, as indicated in Eq. (10). Such a functional can be constructed by summing up a selected class of self-energy diagrams according to the formula³¹

$$\Phi[G] = \sum_{n,k} \frac{1}{2n} \text{tr} \{ \Sigma_k^{(n)} G \}, \quad (\text{A1})$$

where n labels the order of the diagram, i.e., the number of interaction lines, and k labels the distinct self-energy diagrams of that order. The trace is here defined as

$$\text{tr}\{AB\} = \int_0^\beta d\tau \int d\mathbf{r} \int d\mathbf{r}' A(\mathbf{r}, \mathbf{r}'; -\tau) B(\mathbf{r}', \mathbf{r}; \tau). \quad (\text{A2})$$

The systems we consider in this paper consist of electrons interacting with nuclei of charge $\{Z_i\}$ that we treat as fixed-point charges in the positions $\{\mathbf{R}_i\}$, collectively labelled \mathbf{R} . This means that the total energy can be written as $E = E_{\text{el}} + V_{\text{nn}}$, where the nuclear repulsion term is $V_{\text{nn}} = 1/2 \sum_{i,j \neq i} Z_i Z_j / |\mathbf{R}_i - \mathbf{R}_j|$. The electronic term $E_{\text{el}} = T + V_{\text{ne}} + V_{\text{ee}}$ can be obtained from variational functionals of the Green's function (as discussed in, e.g., Ref. 30). Using the finite temperature formalism, it is in fact more convenient to use the thermodynamic grand potential Ω , which is related to the energy through $\lim_{T \rightarrow 0} \Omega = E_{\text{el}} - \mu N$.

For nuclei in fixed positions, the grand potential corresponding to a conserving approximation is a functional¹⁹ of G ,

$$\Omega[G] = \Phi[G] + U_0[G] - \text{tr}\{(GG^{0-1} - 1)\} + \text{tr} \ln\{-G\}, \quad (\text{A3})$$

where $U_0 = 1/2 \int n(\mathbf{r}) v(\mathbf{r} - \mathbf{r}') n(\mathbf{r}')$ is the Hartree energy, and the operator $G^{0-1}(\mathbf{r}_1, \mathbf{r}_2; \tau) = (-\partial_\tau + \nabla^2/2 - w(\mathbf{r}_2; \mathbf{R}) + \mu) \delta(\mathbf{r}_1, \mathbf{r}_2)$. We have here made explicit the dependence of w on the positions of the nuclei, \mathbf{R} . In [Eq. (A3)], all quantities except G^{0-1} are functionals of G , and when G is a self-consistent solution of the Dyson equation, the total energy calculated from this expression will agree with the energy obtained from the method discussed above. An important property of the functional [Eq. (A3)] is that it is stationary,

$$\frac{\delta \Omega[G]}{\delta G} = 0, \quad (\text{A4})$$

when G equals the self-consistent Green's function corresponding to a self-energy $\Sigma = d\Phi/dG$. We now define a Green's function G^λ which depends on the parameter λ according to $G^\lambda(\mathbf{r}, \mathbf{r}'; \tau) = \lambda^3 G(\lambda \mathbf{r}, \lambda \mathbf{r}'; \tau)$. The Green's function $G = G^{\lambda=1}$ is the self-consistent Green's function, and by definition the particle number $N = 2 \text{Tr}\{G^\lambda\}$ is independent of λ .

The proof is now based on the two following points: 1) The variational property [Eq. (A4)] implies that $d\Omega[G^\lambda]/d\lambda = 0$ at $\lambda = 1$. 2) The total energy $E_{\text{el}} + V_{\text{nn}}$ is stationary with respect to changes to the positions of the nuclei when they are in their equilibrium positions, i.e., $dE/d\mathbf{R}_i = 0$. If we consider the λ -dependence of the Hartree energy, we find

$$\begin{aligned} U_0^\lambda &= \frac{1}{2} \int d^3 r \int d^3 r' \frac{n^\lambda(\mathbf{r}) n^\lambda(\mathbf{r}')}{|\mathbf{r} - \mathbf{r}'|} \\ &= \frac{\lambda^6}{2} \int d^3 r \int d^3 r' \frac{n(\lambda \mathbf{r}) n(\lambda \mathbf{r}')}{|\mathbf{r} - \mathbf{r}'|} = \lambda U_0. \end{aligned} \quad (\text{A5})$$

We now consider an n th order term in the Φ functional defined in Eq. (A1). A term $\sum_k^{(n)} [G^\lambda] G^\lambda$ will consist of n interaction lines, $2n$ Green's function lines and integration over $2n$ spatial coordinates. This yields

$$\begin{aligned} &\int d^3 r \int d^3 r' \sum_k^{(n)} [G^\lambda](\mathbf{r}, \mathbf{r}'; \tau) G^\lambda(\mathbf{r}', \mathbf{r}; \tau) \\ &= \lambda^n \int d^3 r \int d^3 r' \sum_k^{(n)} [G](\mathbf{r}, \mathbf{r}'; \tau) G(\mathbf{r}', \mathbf{r}; \tau). \end{aligned} \quad (\text{A6})$$

Summing up all the terms in Eq. (A1), we obtain

$$\left. \frac{d\Phi^\lambda}{d\lambda} \right|_{\lambda=1} = \frac{1}{2} \sum_{n,k} \text{tr}\{\sum_k^{(n)} [G] G\} = U_{\text{xc}}, \quad (\text{A7})$$

where U_{xc} is defined as in Eq. (12).

The term $\text{tr} \ln\{-G^\lambda\}$ is independent of λ . This can be seen by first writing the logarithm as a power series,

$$\text{tr} \ln\{-G^\lambda\} = - \sum_n \frac{1}{n} \text{tr}\{(1 + G^\lambda)^n\} \quad (\text{A8})$$

From the definition of G^λ , it follows that terms on the form $\int d^3 r_1 \dots r_N G^\lambda(\mathbf{r}_1, \mathbf{r}_2; -\tau_1) \dots G^\lambda(\mathbf{r}_N, \mathbf{r}_1; \tau_{N-1})$ are independent of λ , and we therefore have

$$\frac{d \ln \text{tr}\{-G^\lambda\}}{d\lambda} = 0. \quad (\text{A9})$$

Finally, we consider the term $-\text{Tr}\{G^\lambda G_0^{-1}\}$, which translates to

$$\begin{aligned} &\int d\mathbf{r} \left[-\frac{\nabla^2}{2} + w(\mathbf{r}; \mathbf{R}) \right] \rho^\lambda(\mathbf{r}, \mathbf{r}') \Big|_{r'=r} \\ &= \int d\mathbf{r} \left[-\lambda^2 \frac{\nabla^2}{2} + \lambda w(\mathbf{r}; \lambda \mathbf{R}) \right] \rho(\mathbf{r}, \mathbf{r}') \Big|_{r'=r} \end{aligned} \quad (\text{A10})$$

plus terms that are independent of λ . The density matrix is $\rho^\lambda(\mathbf{r}, \mathbf{r}') = \lambda^3 \rho(\lambda \mathbf{r}, \lambda \mathbf{r}')$. The first term on the right hand side is λ^2 times the self-consistent kinetic energy, while the second term equals λ times the electron-nuclear attraction energy, with the position of the nuclei scaled by λ . The derivative is

$$\begin{aligned} &-\frac{d}{d\lambda} \text{Tr}\{GG^{0-1}\} \Big|_{\lambda=1} = 2T + V_{\text{ne}} + \int d^3 r n(\mathbf{r}) \\ &\quad \times \frac{dw(\mathbf{r}; \lambda \mathbf{R})}{d\lambda} \Big|_{\lambda=1}. \end{aligned} \quad (\text{A11})$$

Combining Eqs. (A3), (A5), (A7), and (A11) yields

$$0 = 2T + V_{\text{ne}} + U_0 + U_{\text{xc}} + \int d^3 r n(\mathbf{r}) \frac{dw(\mathbf{r}; \lambda \mathbf{R})}{d\lambda} \Big|_{\lambda=1}. \quad (\text{A12})$$

The electronic energy E_{el} is calculated for nuclei in fixed positions. The energy functional [Eq. (A3)] depends parametrically on the positions \mathbf{R} , and the first order variation in the electronic energy can therefore be written as

$$\delta E_{\text{el}} = \left(\frac{\delta \Omega}{\delta G} \right)_{\{\mathbf{R}_i\}} \delta G + \sum_i \left(\frac{\delta \Omega}{d\mathbf{R}_i} \right)_G \delta \mathbf{R}_i, \quad (\text{A13})$$

where we have used the fact in the zero-temperature limit $d\Omega/d\lambda = dE_{\text{el}}/d\lambda$ and $d\Omega/d\mathbf{R}_i = dE_{\text{el}}/d\mathbf{R}_i$. Because of the variational property [Eq. (A4)], the first term on the right-

hand side of Eq. (A13) disappears, and we only need to consider the second term. In the energy functional [Eq. (A3)], the positions of the nuclei only enter as parameters in the term G^{0-1} , while the Green's function is an independent variable. This means, using Eq. (A13), that

$$\frac{dE_{\text{el}}(\lambda\mathbf{R})}{d\lambda} = - \frac{d \text{tr}\{GG^{0-1}\}}{d\lambda} = \int d^3n(\mathbf{r}) \frac{dw(\mathbf{r};\lambda\mathbf{R})}{d\lambda}. \quad (\text{A14})$$

In equilibrium we have $dE(\lambda\mathbf{R})/d\lambda=0$ at $\lambda=1$. Since $E = E_{\text{el}} + 1/2 \sum_i \sum_{j \neq i} Z_i Z_j / R_{ij}$, where $\mathbf{R}_{ij} = \mathbf{R}_i - \mathbf{R}_j$, we obtain

$$\left(\frac{dE(\lambda\mathbf{R})}{d\lambda} \right)_{\lambda=1} = -V_{\text{nn}} + \int d^3r n(\mathbf{r}) \left. \frac{dw(\mathbf{r};\lambda\mathbf{R})}{d\lambda} \right|_{\lambda=1} = 0. \quad (\text{A15})$$

Equation (A12) then becomes

$$0 = 2T + V_{\text{ne}} + V_{\text{ee}} + V_{\text{nn}}, \quad (\text{A16})$$

which is exactly what we wanted to show: The energies calculated from the Green's function within a conserving approximation satisfy the virial theorem.

¹Y. Xue, S. Datta, and M. A. Ratner, *Chem. Phys.* **281**, 151 (2002).

²E. Runge and E. K. U. Gross, *Phys. Rev. Lett.* **52**, 997 (1984).

³G. Stefanucci and C.-O. Almbladh, *Phys. Rev. B* **69**, 195318 (2004); *Europhys. Lett.* **67**, 14 (2004).

⁴N. D. Lang, *Phys. Rev. B* **52**, 5335 (1995).

⁵L. V. Keldysh, *Zh. Eksp. Teor. Fiz.* **47**, 1515 (1964) [*Sov. Phys. JETP* **20**, 1018 (1965)].

⁶A. L. Fetter and J. D. Walecka, *Quantum Theory of Many-Particle Systems* (McGraw-Hill, New York, 1971).

⁷L. P. Kadanoff and G. Baym, *Quantum Statistical Mechanics* (Benjamin, New York, 1962).

⁸P. Danielewicz, *Ann. Phys.* **152**, 239 (1984).

⁹R. van Leeuwen, *Phys. Rev. Lett.* **76**, 3610 (1996).

¹⁰L. J. Sham and M. Schlüter, *Phys. Rev. Lett.* **51**, 1888 (1983); *Phys. Rev. B* **32**, 3876 (1985).

¹¹D. C. Langreth, *Phys. Rev. Lett.* **52**, 2317 (1984).

¹²R. van Leeuwen and N. E. Dahlen, in *The Electron Liquid Model in Condensed Matter Physics*, edited by G. F. Giuliani and G. Vignale (IOS Press, Amsterdam, 2004).

¹³J. D. Doll and W. P. Reinhardt, *J. Chem. Phys.* **57**, 1169 (1972).

¹⁴J. Linderberg and Y. Öhrn, *Propagators in Quantum Chemistry* (Academic, London, 1973).

¹⁵L. J. Holleboom and J. G. Snijders, *J. Chem. Phys.* **93**, 5826 (1990).

¹⁶L. S. Cederbaum and W. Domcke, *Adv. Chem. Phys.* **36**, 205 (1977).

¹⁷J. V. Ortiz, *J. Chem. Phys.* **103**, 5630 (1995).

¹⁸G. Baym and L. P. Kadanoff, *Phys. Rev.* **124**, 287 (1961).

¹⁹G. Baym, *Phys. Rev.* **127**, 1391 (1962).

²⁰L. S. Cederbaum, G. Hohlneicher, and W. von Niessen, *Chem. Phys. Lett.* **18**, 503 (1973).

²¹B. Holm and U. von Barth, *Phys. Rev. B* **57**, 2108 (1998); P. García-González and R. W. Godby, *Phys. Rev. B* **63**, 075112 (2001).

²²A. Schindlmayr, T. J. Pollehn, and R. W. Godby, *Phys. Rev. B* **58**, 12684 (1998).

²³W. Ku and A. G. Eguiluz, *Phys. Rev. Lett.* **89**, 126401 (2002).

²⁴K. Delaney, P. García-González, A. Rubio, P. Rinke, and R. W. Godby, *Phys. Rev. Lett.* **93**, 249701 (2004).

²⁵D. W. Smith and O. W. Day, *J. Chem. Phys.* **62**, 113 (1975).

²⁶N. E. Dahlen, R. van Leeuwen, and U. von Barth (unpublished).

²⁷P. C. Martin and J. Schwinger, *Phys. Rev.* **115**, 1342 (1959).

²⁸L. Hedin, *Phys. Rev.* **139**, A796 (1965).

²⁹Details on the basis sets are given on request. The basis set used for He is the same as the one used in Ref. 13.

³⁰N. E. Dahlen and U. von Barth, *J. Chem. Phys.* **120**, 6826 (2004); N. E. Dahlen, R. van Leeuwen, and U. von Barth, *Int. J. Quantum Chem.* **101**, 512 (2005).

³¹J. M. Luttinger and J. C. Ward, *Phys. Rev.* **118**, 1417 (1960).

³²N. E. Dahlen and U. von Barth, *Phys. Rev. B* **69**, 195102 (2004).

³³O. Christiansen, J. Olsen, P. Jørgensen, H. Koch, and P.-Å. Malmqvist, *Chem. Phys. Lett.* **261**, 369 (1996).

³⁴C. E. Moore, *Atomic Energy Levels*, Natl. Stand. Ref. Data Ser., NBS Circular No. 467 (U.S. GPO, Washington, DC, 1971).

³⁵K. P. Huber and G. Herzberg, *Constants of Diatomic Molecules, Molecular Spectra and Molecular Structure*, Vol. 4 (Van Nostrand Reinhold, New York, 1979).

³⁶S. G. Lias, R. D. Levin, and S. A. Kafafi, *Ion Energetics Data* in NIST Chemistry WebBook, NIST Standard Reference Database Number 69, Eds. P. J. Linstrom and W. G. Mallard, March 2003, National Institute of Standards and Technology, Gaithersburg MD, 20899 (<http://webbook.nist.gov>).